

Lung vessel segmentation in CT images using graph cuts

Zhiwei Zhai, Marius Staring and Berend C. Stoel

Division of Image Processing, Leiden University Medical Center, Leiden, The Netherlands

ABSTRACT

Accurate lung vessel segmentation is an important operation for lung CT analysis. Hessian-based filters are popular for pulmonary vessel enhancement. However, due to their low response at vessel bifurcations and vessel boundaries, extracting lung vessels by thresholding the vesselness is inaccurate. Some literature turns to graph cuts for more accurate segmentation, as it incorporates neighbourhood information. In this work, we propose a new graph cuts cost function combining appearance and shape, where CT intensity represents appearance and vesselness from a Hessian-based filter represents shape. In order to make the graph representation computationally tractable, voxels that are considered clearly background are removed using a low threshold on the vesselness map. The graph structure is then established based on the neighbourhood relationship of the remaining voxels. Vessels are segmented by minimizing the energy cost function with the graph cuts optimization framework. We optimized the parameters and evaluated the proposed method with two manually labeled sub-volumes. For independent evaluation, we used the 20 CT scans of the VESSEL12 challenge. The evaluation results of the sub-volumes dataset show that the proposed method produced a more accurate vessels segmentation. For the VESSEL12 dataset, our method obtained a competitive performance with an area under the ROC of 0.975, especially among the binary submissions.

Keywords: Graph cuts, vessel segmentation, vesselness, appearance and shape

1. INTRODUCTION

Lung vessel detection is a key research topic in pulmonary CT image processing, since accurate vessel segmentation is an important step in extracting imaging bio-markers of vascular lung diseases. For example, systemic sclerosis (SSc) is related to pulmonary hypertension (PH),¹ which is related to narrowing of the small vessels, and therefore vessel analysis could be used as a bio-marker for PH in SSc. A few methods have been proposed for lung vessel segmentation. According to the VESSEL12 challenge,² the popular Hessian-based methods³ perform well. They enhance tube-like structures by modeling the eigenvalues of the Hessian matrix, but tend to give a low response at the vessel bifurcations and at the vessel boundaries. In our previous work, a strain energy filter⁴ overcomes the bifurcations problems to some degree by analyzing the shape-tuned strain energy density. However, thresholding the strain energy filter's vesselness does not provide accurate results either. In order to improve the vessel segmentation, we turned to graph cuts where we can more easily combine different sources of information via the cost function, and additionally include neighbouring information.

Graph cuts consider the segmentation a labeling problem.⁵ The voxel nodes are labeled to object or background, according to node connections and their weights. Several approaches using graph cuts for vessel segmentation were proposed. Chen et al.⁶ proposed a regional graph cuts based method for liver vessel segmentation with clustering method for initialization. Freiman et al.⁷ proposed a graph cuts based method for carotid artery segmentation by coupling Frangi's vesselness and intensity into the cost function. In order to cope with memory and computational challenges, they divided the scan volume into several regions with a small overlap, computed graph cuts for each block independently, and merged the segmentations.

In this paper, an automatic lung vessel segmentation method based on graph cuts is proposed. A fairly low threshold is applied on the strain energy based vesselness to label voxels that are certainly part of the background, the remaining voxels are included as nodes in the graph. Instead of using vesselness as the vessel data cost term directly,⁷ we take it as a shape feature and compute the vessel data term with a prior distribution. Combining appearance (CT intensity) and shape, the cost function is calculated. To deal with memory requirements, we employed a low overhead sparse matrix implementation to record graph connections and their weights allowing the processing of the entire image volume. After the graph structure is established, the graph cuts optimization framework is applied for vessel segmentation. The proposed lung vessel segmentation method was optimized and evaluated on two manually labeled sub-volumes, and evaluated independently on the VESSEL12 dataset.

2. METHODS

Our segmentation method consists of three steps: 1) the strain energy filter for lung vessels enhancement, 2) the graph structure representation, and 3) the graph cuts based vessels segmentation.

2.1 Vessel enhancement filter

Due to an overly simplified cylindrical model, the response of traditional Hessian-based filters is low at the vessel bifurcations. The strain energy filter, which is based on the strain energy density theory from solid mechanics, aims to remedy this. Based on an intensity continuity assumption, and a relative Hessian strength measure to ensure the dominance of second-order over first-order derivatives to suppress undesired step edges, the final vesselness was calculated as follows:

$$\varphi(\sigma, x) = \begin{cases} 0, & \text{if } \frac{1}{3}(\lambda_1 + \lambda_2 + \lambda_3) > -\zeta\lambda_m \\ \exp\left(-\eta\frac{\|\nabla I\|}{\lambda_m}\right) V^\kappa(x)\rho(H, v), & \text{otherwise,} \end{cases} \quad (1)$$

in which σ is scale, λ_i are the eigenvalues with λ_m the maximum eigenvalue, $\|\nabla I\|/\lambda_m$ measures relative Hessian strength, $V^\kappa(x)$ is a measure for vessel shape and $\rho(H, v)$ measures structure strength. The parameters $0 < \zeta < 1$, $\eta > 0$, $\kappa > 0$ and $-1 < v < 0.5$ are user-defined. More details can be found in the original paper.⁴

2.2 Graph representation

High resolution pulmonary CT scans consist of almost 500 slices per scan, with 512×512 voxels each slice. Considering the lung region only, the graph still consists of almost ten million nodes and hundred million edges (26-neighbours in a 3D grid). To cope with memory requirements, previous work used a block region strategy^{6,7}. However, this introduces discontinuities in the merged part of detected vessels. In this paper, we used a thresholding strategy to reduce the graph size.

A fairly low threshold was used on the vesselness to label voxels as background. The nodes of the graph consist of the remaining voxels, source and sink nodes. The edges between the source/sink node and voxel nodes are called t-edges, and the edges between neighbourhood voxel nodes are named n-edges. The t-edges and their weights can be represented easily with a dense matrix. For the n-edges, a sparse matrix was adopted to record the adjacent connections and their weights. If we use '1' and '0' to represent the 'connection' and 'non-connection' of the voxels respectively, all the '1' locate at the several parallel diagonals of the sparse matrix. The adjacent sparse matrix can be determined efficiently and memory-saving by assigning the diagonal vectors. The diagonal vectors can be generated easily by analyzing the neighbour connection type. Then, the n-edge's sparse matrix can be extracted from the whole 3D grid adjacent sparse matrix with remaining voxels' index.

2.3 Proposed cost function for the graph cut

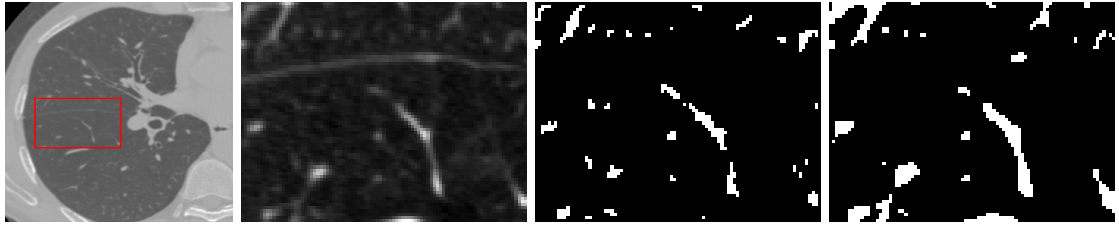
Segmentation is treated as a labeling problem by graph cuts, $L = \{L_p | p \in \mathcal{P}\}$. The proposed energy function is:

$$E(L) = \sum_{p \in \mathcal{P}} (wD_p^{CT}(L_p) + (1-w)D_p^{vsl}(L_p)) + \gamma \sum_{(p,q) \in \mathcal{N}, L_p \neq L_q} V_{p,q}(L_p, L_q), \quad (2)$$

where the data term consists of appearance (CT intensity) $D_p^{CT}(L_p)$ and shape (vesselness) $D_p^{vsl}(L_p)$, and w is the balance weight. $V_{p,q}(L_p, L_q)$ is the cost of the edge (p, q) and γ is a user-defined positive coefficient for adjusting the smoothness.

Commonly Gaussian functions are used in the data term,⁷ but this will cause voxels with high intensity or vesselness, i.e. far away from the center of the Gaussian, to obtain a low vessel probability. Therefore we employed a sigmoid function:

$$D_p^{CT}(I_p | L_p = l) = \frac{1}{1 + e^{-\alpha_l^{CT}(I_p - \beta_l^{CT})}}; \quad D_p^{vsl}(I_p | L_p = l) = \frac{1}{1 + e^{-\alpha_l^{vsl}(I_p - \beta_l^{vsl})}}. \quad (3)$$



(a) Original CT slice (b) Slice of sub-volume (c) Reference standard (d) Graph cuts result

Figure 1. Segmentation result on reference region. (a) reference region. (b) one slice of the extracted region. (c) manually segmented reference standard. (d) segmentation result of our proposed method.

The choice for the free parameters of the sigmoid function is given in Section 3.1. The boundary cost $V_{p,q}(L_p, L_q)$ is based on the similarity in appearance of neighbouring voxels p and q , weighted by their spatial distance:

$$V_{p,q}(L_p, L_q) = \begin{cases} e^{-\frac{|I_p - I_q|}{\text{dist}(p,q)}}, & \text{if } L_p \neq L_q \text{ and } (p, q) \in \mathcal{N} \\ 0, & \text{otherwise} \end{cases} \quad (4)$$

If two nodes of the n-edge (p, q) have similar appearance but a different label, the edge’s boundary cost will be high.

3. EXPERIMENTS AND RESULTS

3.1 Parameter estimation

The parameters used in the strain energy vesselness filter were taken from the literature:⁴ $\zeta = 0.5$, $\eta = \kappa = 0.2$, $v = 0.0$, and using scales $\delta \in \{1, 2, 3\}$. The parameters in the graph cuts energy function were optimized with sub-volumes data, γ was set to 0.01, the weight w in Eq.(2) was 0.6. For the sigmoid cost function’s parameters, we designed an algorithm to estimate them automatically. Before estimation, we removed voxels which have high vesselness or intensity, because those voxels can affect the distribution estimation severely. Afterwards, a threshold was used to set the initial background and foreground. The Gaussian distribution of the intensity in the foreground is estimated by the mean μ and the standard deviation std of the initial foreground. Then, we fitted the sigmoid function to the unnormalized Gaussian such that $Sigmoid(\beta) = Gaussian(\beta) = 0.5$. For estimating the fuzziness parameter α we did several experiments and finally found that the best fitting curve was obtained by: $Sigmoid(\mu) = 0.95$.

3.2 Data and results

In order to evaluate the proposed segmentation method, we chose two sub-volumes across the boundary of pulmonary lobes for manual annotation by an expert (see Figure 1). In total, two reference standard sub-volumes from different patients, Dataset1 with size $65*60*120$ and Dataset2 with size $91*70*121$, were extracted.

Centerline-based evaluation was applied to these two sub-volumes dataset. The centerlines were extracted from segmented vessels with the 'DtfSkeletonization' module in MeVisLab. The centerline of the segmentation result was compared with the centerline of the reference standard. If the distance between the two centerlines are less than the local vessel radius, they were counted as true positives. The number of false negatives was calculated as the number of voxels on the reference standard centerline minus the number of true positives. The number of false positives was calculated using the number of voxels on the segmented centerlines minus the number of true positives. Then the precision, recall and F1 score, $F1 = 2TP/(2TP + FP + FN)$, were calculated. We compared the proposed method with thresholding the Frangi’s vesselness, thresholding the strain energy filter’s vesselness and a Freiman’s based method.⁷ For the thresholding vesselness methods, 70 thresholds were evaluated ranging between the minimum and maximum of vesselness, and the optimized results of the filters are given in Table 1.

For independent evaluation, we used the VESSEL12 dataset of 20 anonymized CT scans from three hospitals, representing a wide range of clinical images. The manual labelling was performed on pre-generated points, and

Table 1. Evaluation results on the sub-volumes dataset

	Dataset1			Dataset2		
	Recall	Precision	F1 score	Recall	Precision	F1 score
Frangi filter ³	0.734	0.508	0.601	0.629	0.515	0.566
Freiman’s based method ⁷	0.823	0.478	0.605	0.643	0.487	0.554
Strain Energy filter ⁴	0.708	0.729	0.718	0.622	0.712	0.664
Our method	0.733	0.792	0.761	0.667	0.715	0.690

Table 2. Evaluation results of the VESSEL12 dataset: Az score, Specificity and Sensitivity of our submission across all categories. Categories 1: Principal, 2: Small Vessels, 3: Medium Vessels, 4: Large Vessels, 5: Vessel/Airway Wall, 6: Vessel/Dense Lesion, 7: Vessel/Mucus-filled bronchi, 8: Vessel-in-lesion/Lesion, 9: Vessel/Nodules.

	1	2	3	4	5	6	7	8	9
Az	0.975	0.953	0.977	0.993	0.867	0.481	0.331	0.661	0.238
Specificity	0.910	0.865	0.910	0.979	0.588	0.239	0.112	0.451	0.038
Sensitivity	0.929	0.966	0.953	0.960	0.929	0.929	0.929	0.829	0.929

only those points were included for which the labels from three independent observers are the same. The segmentation vessels were evaluated against the manual annotations. We submitted our binary vessel segmentations to VESSEL12 organizers, and our method obtained an area under the ROC (Az) of 0.975, which is a competitive performance on VESSEL12, especially among the binary submissions. The evaluation results of our method is shown in Table 2; the evaluation results of other submissions can be found in the paper.²

4. CONCLUSION AND DISCUSSION

A graph cuts based segmentation method is proposed to extract lung vessels. By combining appearance and shape features, a new data term cost function was designed. An efficient and accurate strategy was adopted to cope with memory requirements of a graph representation. From the evaluation results, we obtained a competitive performance. The method could be improved by adding more information, such as the inclusion of radius information in the data term and by designing a more accurate boundary cost using differences in multiple features. The airway wall and nodule removal could improve the performance by reducing the false positives.

REFERENCES

1. E. Hachulla, V. Gressin, L. Guillevin, *et al.*, “Early detection of pulmonary arterial hypertension in systemic sclerosis: a French nationwide prospective multicenter study,” *Arthritis & Rheumatism* **52**(12), pp. 3792–3800, 2005.
2. R. D. Rudyanto, S. Kerkstra, E. M. Van Rikxoort, *et al.*, “Comparing algorithms for automated vessel segmentation in computed tomography scans of the lung: the VESSEL12 study,” *Medical image analysis* **18**(7), pp. 1217–1232, 2014.
3. A. F. Frangi, W. J. Niessen, K. L. Vincken, and M. A. Viergever, “Multiscale vessel enhancement filtering,” in *Medical Image Computing and Computer-Assisted Intervention*, pp. 130–137, Springer, 1998.
4. C. Xiao, M. Staring, D. Shamonin, J. H. Reiber, J. Stolk, and B. C. Stoel, “A strain energy filter for 3D vessel enhancement with application to pulmonary CT images,” *Medical image analysis* **15**(1), pp. 112–124, 2011.
5. Y. Boykov and V. Kolmogorov, “An experimental comparison of min-cut/max-flow algorithms for energy minimization in vision,” in *Energy minimization methods in computer vision and pattern recognition*, pp. 359–374, Springer, 2001.
6. B. Chen, Y. Sun, and S. H. Ong, “Liver vessel segmentation using graph cuts with quick shift initialization,” in *The 15th International Conference on Biomedical Engineering*, pp. 188–191, Springer, 2014.
7. M. Freiman, N. Broide, M. Natanzon, *et al.*, “Vessels-cut: a graph based approach to patient-specific carotid arteries modeling,” in *Modelling the Physiological Human*, pp. 1–12, Springer, 2009.